

1 **Supporting Information: MATERIALS AND METHODS**

2

3 *Mesocosm setup*

4 Upon filling of the containers and arrival of the seawater to the CRETACOSMOS mesocosm
5 facilities (<http://cretacosmos.eu/>), we evenly distributed the water to 9 food grade polyethylene
6 mesocosm bags to a final volume of 3 m³ by gravity siphoning with acid cleaned and deionized
7 rinsed plastic tubes. The seawater had been transported to the facilities within maximum one
8 hour from sampling, and the mesocosms were deployed in a large concrete tank (350 m³) and
9 incubated at *in situ* temperature, which was constantly regulated by a continuous flow system.
10 With an airlift system that was deployed inside the mesocosms, we ensured a gentle mixing of
11 the water column and avoided stratification. Plexiglas lids were attached to the top of the
12 mesocosms to avoid contamination by aerosols. During all mesocosm handlings, gloves were
13 used to avoid contamination, while the lid was opened only when necessary with silicone tubes
14 hanging outside the mesocosms and kept clean at all times.

15

16 *Materials for silver nanoparticle determination*

17 Dowex®1 X-8 chloride form styrene-divinyl benzene cross-linked resin with tertiary amine
18 moieties (Sigma-Aldrich) and Amicon Ultra 3k (Millipore) membrane insert for centrifugal
19 device with a membrane cutoff of 3 KDa were employed as received. We used silver
20 nanoparticles capped with branched-poly(ethyleneimine) (BPEI) with a nominal diameter of 60
21 nm (Nanocomposix, NanoXact, San Diego, CA, 99.99% silver purity).

22

23 *Determination of silver nanoparticles*

24 The inductively coupled plasma mass spectrometer (ICP-MS) instrument used in this study
25 was a NexION 300X ICP-MS (PerkinElmer, Shelton, CT, U.S.A.) set with a 10 msec dwell

26 time for AgNP analysis of either isotope ^{107}Ag or ^{109}Ag . Sub-samples were analyzed using flow
 27 injection on-line dilution ICP-MS in single particle mode (FI spICP-MS). This was achieved
 28 by introducing seawater samples without any pre-treatment via a fused silica capillary (100 μm
 29 i.d. and 200 μm o.d.) and a 20 μL injection loop. Online dilution of the seawater samples
 30 flowing at 10 $\mu\text{L min}^{-1}$ was achieved by mixing with a deionized water makeup flow at 0.8 mL
 31 min^{-1} approximately 3-5 mm before the tip of a conventional pneumatic nebulizer (Meinhard
 32 Type C nebulizer, Meinhard). An Eksigent ekspert™ Ultra High Performance nanoLC 425
 33 pump system (Eksigent part of AB SCIEX Dublin, CA) was used to deliver carrier flow rates
 34 of 10 $\mu\text{L min}^{-1}$. In order to determine the mass of the analyte per NP (g) present in seawater
 35 samples, the system was calibrated by analyzing a standard seawater suspension containing
 36 AgNPs of known size (60 nm) at 200 ng Ag L^{-1} , thus of known number concentration (NPs L^{-1})
 37 and mass of Ag per NP (m_{AgNP}^{std}) (derived from transmission electron size data; Table S1).
 38 The latter is related to the determined average spike intensity (\bar{q}_{AgNP}) for the standard NPs from
 39 4 injections (20 μL each) through the k response, factor as shown in equation 1. Transformation
 40 of equation 1 to 2 allowed for the k response factor determination.

$$41 \quad m_{AgNP}^{std} = k \cdot \bar{q}_{AgNP} \quad (1)$$

$$42 \quad k = \frac{m_{AgNP}^{std}}{\bar{q}_{AgNP}} \quad (2)$$

43 Subsequently, the k factor was used to calculate the mass of Ag for each individual NP
 44 detected in the seawater samples ($m_{i, AgNP}$) from their determined spike intensity ($q_{i, AgNP}$)
 45 using equation 3, where i represents individual NPs:

$$46 \quad m_{i, AgNP} = k \cdot q_{i, AgNP} \quad (3)$$

47 Based on the assumption that the NPs are spherical, as they were when spiked in the seawater,
 48 their individual sizes were determined using equation 4:

$$49 \quad d_{i, AgNP} = \sqrt[3]{\frac{6m_{i, AgNP}}{\pi \rho}} \quad (4)$$

50 where ρ is the density of the analyte metal (10.49 g cm⁻³ for Ag). The determined NP sizes (
51 $d_{i,AgNP}$) were then size binned (5 nm size bins) and their resulting size distribution histograms
52 were plotted. The individual NP diameter values were also used to determine average AgNP
53 diameters (\bar{d}_{AgNP}) for each of the analyzed seawater samples. Finally, in order to determine the
54 AgNP number concentration the nebulization efficiency ε_n was calculated in the FI mode, using
55 equation 5:

$$56 \quad \varepsilon_n = \frac{n_{det}}{n_{inj}} \quad (5)$$

57 Where n_{det} is the number of detected AgNP pulses and n_{inj} is the number of NPs injected
58 for a standard seawater suspension containing AgNPs of known number concentration.

59 The number of injections for each sample (3-4) varied depending on the total number of
60 detected NPs in order to adequately determine their size distribution. Each injection resulted in
61 data files consisting of 50000 data points (10 msec each).

62 In order to clean the injection valve, loop and capillary tubing, between each sample type, a
63 cleaning solution consisting of 3% w/w nitric acid and 3% w/w hydrogen peroxide was passed
64 through the injector and the connecting capillaries to the nebulizer at a flow of 2,0 $\mu\text{L min}^{-1}$ (for
65 additional details about system cleaning see supplementary information section).

66

67 *Determination of dissolved Ag⁺ in seawater samples*

68 Part of the aliquots collected for AgNP analysis were placed in an 1.5-mL tube and
69 centrifuged with an insert centrifugal filtering device with a membrane cutoff filter of 3 kDa
70 for 3 min at 10.000 rpm. Then, 5.0±0.3 mg of Dowex® 1-X8 strong base anion exchange resin
71 (styrene divinylbenzene co-polymer with tertiary amines as functional group) was placed in an
72 eppendorf tube with 0.5 mL of 3 kDa-filtered sample and 0.1 mL of 0.6 M HCl. After 2 min of
73 vortexing, the suspension was centrifuged for 2 min at 10.000 rpm and the supernatant was
74 removed. Deionized water (500 μL) was added to the solid content. After another 2 min of

75 vortexing, the suspension was centrifuged for 2 min at 10.000 rpm and the supernatant was
76 removed. Finally, 0.2 mL of 4% w/v nitric acid was added to the solid sample in order to recover
77 the pre-concentrated dissolved Ag. After 2 min of vortexing and centrifuging for 2 min at
78 10.000 rpm, the supernatant was collected and analyzed directly via ICP-MS with a dwell time
79 of 100 msec (conventional ICP-MS conditions). Samples were up taken directly by the
80 nebulizer in continuous mode. The calibration was performed by using the same method with
81 known concentration of dissolved Ag in deionized water in the range of concentration expected
82 for the unknown samples (i.e. 0, 50, 500 and 1000 ng Ag L⁻¹). The signal areas after blank
83 subtraction were employed for calibration line construction ($R^2=0.996$).

84

85 *Determination of total Ag in 0.2, 2.0 and 5.0 µm filters*

86 AgNP integrity throughout the sonication treatment was demonstrated by analyzing a
87 standard seawater solution that had been spiked with AgNP and sonicated for 10 min with the
88 same conditions as above ¹. Total Ag concentration of 5.0 µm filters were determined using a
89 modification of the method described by USEPA Method ² for microwave assisted acid
90 digestion of siliceous and organically based matrices. Acid-cleaned Teflon vessels and a closed
91 high pressure microwave system (Multiwave 3000, Anton Paar, Austria) were used for the
92 digestion. For 5.0 µm filters, 2 ml of concentrated H₂O₂ (≥30%, TraceSELECT® Ultra, for
93 ultratrace analysis), 6 ml of concentrated HNO₃ (TraceSELECT®, for trace analysis, ≥69.0%)
94 were added and the vessels were sealed and transferred to the microwave system where they
95 remained for 50 min. After digestion, samples were evaporated in a closed evaporation system
96 in a sandbath at 125 °C. At incipient dryness, samples were cooled and transferred with 0.67
97 mL HCl (≥67%) and 5% HNO₃ (≥69.0%) into 25 mL volumetric flasks. Samples were stored
98 in polypropylene sample bottles at 4 °C until analysis with ICP-MS (NexION300, PerkinElmer,
99 Shelton, CT, U.S.) was conducted.

100

101 *Determination of additional chemical parameters*

102 The detection limits for phosphate, nitrate and ammonium concentration analyses were
103 0.0137, 0.0168 and 0.0187 μM , respectively.

104 We measured total organic carbon concentration using a TOC 5000 Shimadzu analyzer^{3,4}.
105 Precision and accuracy of the measurements was tested against Florida Strait Seawater
106 Reference Material provided by the DOC-CRM program, batch 10 FS-2008 (University of
107 Miami - D.A. Hansell); measured value: $44 \pm 2 \mu\text{mol C L}^{-1}$ $n=2$, certified value: 41-44 $\mu\text{mol C}$
108 L^{-1} .

109 We measured the concentration of particulate organic carbon and nitrogen using a Perkin
110 Elmer 2400 CHN Elemental Analyzer.

111 Filters for chlorophyll *a* concentration (Chl *a*) analysis were extracted in 90% acetone at 4°C
112 in the dark overnight. We then determined Chl *a* concentration using a Turner TD-700
113 fluorometer and the sum of the three size fractions (0.2-2.0, 2.0-5.0, and $>5 \mu\text{m}$) was calculated.
114

115 *Determination of production rates*

116 For primary production (PP) measurement, we filled two light and one dark 320-mL
117 polycarbonate bottles with water from the microcosms in the morning, inoculated them with 5
118 μCi of $\text{NaH}^{14}\text{CO}_3$ tracer and then incubated them in the land-based tank for approximately 3
119 hours. At the end of the incubation time, replicate bottles were immediately filtered through 0.2
120 and 2.0 μm 47 mm polycarbonate filters. All filtrations were performed under low vacuum
121 pressure. In order to remove excess ^{14}C -bicarbonate, we soaked filters in 1 mL 0.1 N HCl and
122 left them in open polyethylene 5-mL vials overnight. After adding 4 mL of scintillation cocktail,
123 radioactivity was measured in a scintillation counter. The fraction of 0.2-2.0 μm corresponded
124 to pico- and the fraction of $>2.0 \mu\text{m}$ corresponded to nano- and micro- planktonic PP rates, and
125 are presented as percentages (% pico and % nano/micro PP). The incubations were generally
126 done around midday when incident light was at its greatest and the incubation area received the

127 same light intensity as the mesocosms. For the concentration of dissolved inorganic carbon and
128 the isotopic discrimination factor we used the values 26.400 mg C m⁻³ and 1.05, respectively.

129 For heterotrophic bacterial production (BP) measurement, two replicated seawater samples
130 (1.5 mL) and one trichloroacetic acid (TCA)-killed control were incubated in 2 mL-tubes with a
131 mixture of [4,5-³H] leucine (Perkin Elmer, specific activity 115 Ci mmol⁻¹) and nonradioactive
132 leucine at final concentrations of 16 and 7 nM, respectively. We incubated all samples,
133 including controls, for 2 h in the dark at *in situ* temperature, based on daily temperature
134 measurements. Incubation was terminated with the addition of 90 µL of 100% TCA. We then
135 stored the samples at 4 °C in the dark until further processing. Centrifugation was carried out at
136 16000 g for 10 min. After discarding the supernatant, 1.5 mL of 5% TCA was added, samples
137 were vigorously shaken using a vortex and then centrifuged again at the same speed. After
138 discarding the supernatant, 1.5 mL of 80% ethanol was added, and then samples were shaken
139 and centrifuged again. The supernatant was discarded and 1.5 mL of scintillation liquid was
140 added. The radioactivity incorporated into the pellet was counted using a Liquid Scintillation
141 Counter (Packard LS 1600). BP was calculated from the ³H-leucine incorporation rates ⁵. We
142 carried out a times-series experiment to show that the incorporation was linear with time and
143 we performed two kinetic experiments to verify that the concentration of added leucine was
144 sufficient to saturate incorporation. The results of the kinetics showed that the degree of
145 participation of 20 nM used was always >90%, thus the isotopic dilution was negligible.

146

147 *Determination of plankton abundances*

148 Virus-like particles (VLP) and heterotrophic bacteria (HB) were diluted in Tris-EDTA buffer
149 solution (pH=8, Sigma-Aldrich) to maintain particles' enumeration at a rate of <1000 events
150 sec⁻¹. Both VLP and HB were stained with SYBR Green I (Molecular Probes) at a 5x10⁻⁵ and
151 4x10⁻⁴ final dilution of the stock solution, respectively and incubated for 10 min at 80 °C and
152 for 10 min in the dark, respectively. We further distinguished VLP and HB in categories based
153 on their fluorescence signals (i.e. DNA content). We used yellow-green latex beads of 1 µm

154 nominal size (Polysciences) as an internal standard of fluorescence. Autotrophic and
155 heterotrophic nano- and heterotrophic pico- eukaryotes were stained with SYBR Green I
156 (Molecular Probes) at a 2×10^{-4} final dilution of the stock solution and incubated for 60 min in
157 the dark at room temperature. Autotrophs were discriminated from heterotrophs in the green
158 vs. red fluorescence plots. We used yellow-green latex beads of 1 and 10 μm nominal size
159 (Polysciences) as internal standards of fluorescence. The flow rate of the instrument was daily
160 determined and used for abundance conversion, by accurately weighing a trial TRIS-EDTA
161 buffer solution sample before and after running for 5 min at high-speed performance.

162

163 *Determination of reactive oxygen species*

164 We stained untreated samples with H_2DCFDA (50 μM final concentration), incubated them
165 for 60 min in the dark and then analyzed them in the same FACSCalibur™ flow cytometer, as
166 above. Control samples (Milli-Q water) were also stained and used to subtract the background
167 noise.

168

169 *Determination of bacterial viability*

170 Immediately after collection, samples were simultaneously stained and incubated with the
171 fluorescent dye SYBR Green I (Molecular Probes, final concentration 4×10^{-4}) and the
172 fluorescent dye propidium iodide (PI, Molecular Probes, final concentration: 50 $\mu\text{g mL}^{-1}$). We
173 incubated samples at room temperature in the dark for 20 min. An additional sample was stained
174 with SYBR Green I only and used to subtract “dead” from total bacterial cells. The percentage
175 of “live” (i.e. viable and membrane-compromised) and “dead” (i.e. membrane-damaged) cells
176 is presented over the total bacterial abundance.

177

178 *DNA extraction, amplification and sequencing*

179 Frozen 0.2- μm filters were grinded with a mortar and pestle in a continuous flow of liquid
180 nitrogen. Grinded filters were incubated at 60 °C for 2 hours at 2 turns min^{-1} with 10 mL CTAB
181 buffer [2% CTAB (hexadecyltrimethylammonium bromide); 100 mM TrisHCl (pH=8); 20 mM
182 EDTA; 1.4 M NaCl; 0.2% β -mercaptoethanol; 0.1 mg mL^{-1} proteinase K; 10 mM DTT
183 (dithiothreitol)]. DNA was purified using equal volume of chloroform:isoamylalcohol solution
184 (24:1), followed by centrifuge at 75000 rpm for 10 min at 4 °C. The aqueous phase was treated
185 with RNase and the chloroform:isoamylalcohol step was repeated. DNA was then precipitated
186 with a 2/3 volume of isopropanol overnight, followed by centrifuge at 75000 rpm for 15 min at
187 4 °C to pellet DNA. Pellet was washed with 76% v/v ethanol and 10 mM ammonium acetate
188 solution. The extracted DNA was dissolved in ultrapure water and stored at -20 °C until PCR
189 amplification and sequencing. Bacterial DNA was quantified with a 3.0 QubitTM fluorometer
190 (Thermo Fisher) and its quality was assessed with a NanoDrop spectrophotometer (ND-100,
191 Thermo Scientific) and by agarose gel electrophoresis.

192 We used a two-step PCR protocol; the first PCR reactions for the 16S rRNA gene with the
193 locus-specific primers (341f: 5-CCTACGGGNGGCWGCAG-3 and 805RB: 5-
194 GACTACNVGGGTATCTAATCC-3) and a universal 5' tail specified by Illumina contained
195 the DNA template, PCR buffer with dNTPs mixture (10x AccuPrimeTM PCR buffer II), forward
196 and reverse primers (10 μM) and AccuPrimeTM Taq high fidelity DNA polymerase (1 unit).
197 DNA template concentration was approximately 50 ng μL^{-1} . The PCR protocol used was: 98
198 °C for 3 min; 28 cycles at 98 °C for 30 sec; 55 °C for 30 sec; 72 °C for 30 sec; 72 °C for 5 min.
199 The second PCR was done with primers that included the indexes and the Illumina adaptors
200 and it contained the clean DNA template, PCR reaction buffer (5x Q5, New England
201 BioLabs®), dNTPs mixture (10mM), forward and reverse primers (10 μM) and Q5® high
202 fidelity DNA polymerase (0.02 unit μL^{-1}). The PCR protocol used was: 98 °C for 3 min; 8
203 cycles at 98 °C for 30 sec; 55 °C for 30 sec; 72 °C for 30 sec; 72 °C for 5 min. First-PCR product
204 was cleaned up using the illustraTM ExoProStarTM PCR and Sequence reaction clean-up kit,
205 following manufacturer instructions. The SequalPrepTM Normalization plate kit was used to

206 purify and normalize second-PCR products, following manufacturer instructions. Pooled PCR
207 products were run in an Agilent 2100 Bioanalyzer (Agilent Technologies). Negative controls
208 in all PCRs were included. PCR products presence and length were ascertained by gel
209 electrophoresis in 1% w/v agarose gel.

210 For viral particle flocculation, 1 mg L⁻¹ FeCl₃ solution was prepared the day of the sampling
211 and kept at room temperature in the dark. Upon chemical treatment, vigorous mixing of the 0.2-
212 µm filtrate followed. Virus particles were let to flocculate for 6-10 hours and then collected on
213 1 µm 142 mm polycarbonate filters, which were stored at 4 °C in the dark pending re-
214 suspension. Viral particle re-suspension from the filters was done as in ⁶ with ascorbic acid
215 buffer. Briefly, a solution of ascorbate-EDTA buffer was prepared daily (0.25 M ascorbic acid,
216 0.2 M Mg₂EDTA, pH 6–7 adjusted with Tris HCl and NaOH), kept in the dark and added in
217 the viral flocculate, followed by shaking by hand and rotation overnight at 4 °C. After re-
218 suspension, viral particles in liquid were retained from the filter by low-speed centrifuge. We
219 followed the same protocol for viral DNA extraction as for bacterial DNA extraction described
220 above. For viral DNA quantification the Qubit® high sensitivity assay kit was used in a 3.0
221 Qubit™ fluorometer (Thermo Fisher), and subsequently, replicates of the three mesocosms
222 were pooled in order to increase the concentration for whole virome sequencing. Viral DNA
223 shearing was done at 300 bp using the standard protocol for Covaris focused ultra-sonicator.
224 An indexed library for Illumina sequencing was prepared using the NEBNext Ultra DNA
225 Library Prep Kit for Illumina (New England BioLabs®), following manual instructions. Size
226 selection was done using AMPure® XP beads and PCR cycles were 6 following manufacturer
227 conditions, with regards to the amount of DNA input. The amount and size distribution of the
228 pooled product were determined with Qubit® high sensitivity assay kit and Agilent 2100
229 Bioanalyzer (Agilent Technologies), respectively, as described above. Library preparation of
230 viral metagenomes was done with the NEBNext Ultra DNA Library Prep Kit for Illumina,
231 following manufacturer instructions.

232 Viral metagenomic libraries were prepared with the NEBNext Ultra DNA Library Prep Kit
233 for Illumina (New England Biolabs) according to the manufacturer's instructions. Metagenomic
234 DNA (500 – 1.000 ng per sample) was previously sheared down to ~200 bp using a Covaris™
235 system and the appropriate time protocol, and size selection was applied after the Illumina
236 adaptors were ligated using AMPure XP Beads (Beckman Coulter). Metagenomic libraries
237 were sequenced in the Illumina HiSeq 4000 platform available at KAUST Bioscience Core Lab
238 using paired-end sequencing.

239

240 *Sequence analyses*

241 The raw 16S rRNA sequences were quality-checked and analysed using both UPARSE v82
242 and QIIME v1.93. Paired-end reads were formed with the fastq-join algorithm
243 (<https://code.google.com/p/ea-utils/wiki/FastqJoin>), by assembling the raw forward and reverse
244 reads of each sample with a minimum overlap of 50 nucleotides and a maximum of one
245 mismatch within the overlapping region. The quality of the paired reads was then checked in
246 QIIME, the forward and reverse primers were removed from the sequence ends of the high-
247 quality reads and the individual sample files were merged. The single file that contained all
248 sample reads was then imported in UPARSE where operational taxonomic units (OTUs) of
249 97% sequence similarity were picked and chimeric sequences were further discarded by de-
250 novo and reference-based detection. For reference-based detection, the “Gold” database
251 (<http://microbiomeutil.sourceforge.net/>) was used. The representative sequences of the OTUs
252 were then assigned taxonomy in QIIME with UClust4 and searching against the newest
253 Greengenes database⁵. Rarefaction curves were drawn indicating that the diversity in all
254 samples was adequately covered (Fig. S4). Finally, the OTU counts for each sample and the
255 taxonomic assignments were combined into an OTU table. OTUs that were taxonomically
256 affiliated to Archaea and OTUs without a taxonomic assignment were further removed from
257 subsequent analyses. The resulting OTU table was used as an input for alpha- and beta-diversity
258 analyses.

259 Metagenome reads in FASTQ format were imported to CLC Genomics Workbench v.7 (CLC
260 Bio) and trimmed using a minimum phred score of 20, a minimum length of 50 bp, allowing
261 no ambiguous nucleotides and trimming off Illumina sequencing adaptors if found. The
262 trimmed metagenome reads were assembled using CLC's *de novo* assembly algorithm, using a
263 k-mer of 63 and a minimum scaffold length of 500 bp. The assembled contigs were then
264 analyzed using the iVirus pipeline ⁷ through the Cyverse platform ⁸. Briefly, viral contigs were
265 identified using the VirSorter software, which classifies viral and prophages sequences with
266 three levels of confident predictions. We only considered the first two levels for the rest of the
267 analysis. The VirSorter software also assigns functions and taxa to the viral contigs. The
268 vContact software was then used to perform guilt-by-contig-association automatic
269 classification of viral contigs and to clusters proteins. Normalization was done using the results
270 of the viral flow cytometry (Fig. 2d). Shannon's diversity index and Pielou's evenness were
271 calculate on all viral proteins and on protein clusters with more than two predicted ORFs using
272 the vegan package in R ^{9,10}. Further proteins annotations were done with the viral Orthologs
273 groups of the eggNOG database ¹¹. The list of auxiliary metabolic genes (AMGs) was obtained
274 from ¹². The AMGs were observed by blasting the trim reads with the diamond software ¹³ with
275 an e-value < 10⁻⁶ against a recent database of AMGs related to cyanobacterial photosynthesis
276 ¹². The results were then normalized with the viral count for each sample obtained by flow
277 cytometry (Fig. 2d). Proteins sequences were downloaded using the UNIPROT database
278 (UniProt Consortium, 2014) and blasted against the viral proteins (e-value 1e⁻⁶, min 60 % of
279 identity). As in ¹⁴, phage attachment site (attP) that are exact match to bacterial tRNA gene
280 (attB) ¹⁵ were obtained by blasting the viral contigs against the tRNADB-CE database ¹⁶ (min
281 100% of identity).

282

283 **References**

- 284 1. Toncelli, C., Mylona, K., Tsapakis, M. & Pergantis, S. A. Flow injection with on-line
285 dilution and single particle inductively coupled plasma-mass spectrometry for

- 286 monitoring silver nanoparticles in seawater and in marine microorganisms. *J. Anal. At.*
287 *Spectrom.* (2016). doi:10.1039/C6JA00011H
- 288 2. 3052, M. Microwave assisted acid digestion of siliceous and organically based
289 matrices. 1–20 (1996).
- 290 3. Cauwet, G. HTCO method for dissolved organic carbon analysis in seawater:
291 influence of catalyst on blank estimation. *Mar. Chem.* **47**, 55–64 (1994).
- 292 4. Sugimura, Y. & Suzuki, Y. A high-temperature catalytic oxidation method for the
293 determination of non-volatile dissolved organic carbon in seawater by direct injection
294 of a liquid sample. *Mar. Chem.* **24**, 105–131 (1988).
- 295 5. Kirchman, D. Measuring Bacterial Biomass Production and Growth Rates from
296 Leucine Incorporation in Natural Aquatic Environments. *methods Microbiol.* **30**, 227–
297 237 (1993).
- 298 6. John, S. G. *et al.* A simple and efficient method for concentration of ocean viruses by
299 chemical flocculation. *Environ. Microbiol. Rep.* **3**, 195–202 (2011).
- 300 7. Bolduc, B., Youens-Clark, K., Roux, S., Hurwitz, B. L. & Sullivan, M. B. iVirus:
301 Facilitating new insights in viral ecology with software and community data sets
302 imbedded in a cyberinfrastructure. *ISME J.* **11**, 7–14 (2017).
- 303 8. Goff, S. A. *et al.* The iPlant Collaborative: Cyberinfrastructure for Plant Biology.
304 *Front. Plant Sci.* **2**, 1–16 (2011).
- 305 9. Brum, J. R. *et al.* Patterns and ecological drivers of ocean viral communities. *Science*
306 *(80-)*. **348**, 1–10 (2015).
- 307 10. Oksanen, J. *et al.* Community Ecology Package, Package ‘vegan’. (2017). doi:ISBN
308 0-387-95457-0
- 309 11. Huerta-Cepas, J. *et al.* EGGNOG 4.5: A hierarchical orthology framework with

- 310 improved functional annotations for eukaryotic, prokaryotic and viral sequences.
311 *Nucleic Acids Res.* **44**, D286–D293 (2016).
- 312 12. Hurwitz, B. L. & Ren, J. M. U. Viral metabolic reprogramming in marine ecosystems.
313 *Curr. Opin. Microbiol.* **31**, 161–168 (2016).
- 314 13. Buchfink, B., Xie, C. & Huson, D. H. Fast and sensitive protein alignment using
315 DIAMOND. *Nat. Methods* **12**, 59–60 (2014).
- 316 14. Bellas, C. M., Anesio, A. M. & Barker, G. Analysis of virus genomes from glacial
317 environments reveals novel virus groups with unusual host interactions. *Front.*
318 *Microbiol.* **6**, 1–14 (2015).
- 319 15. Mizuno, C. M., Rodriguez-valera, F., Kimes, N. E. & Ghai, R. Expanding the Marine
320 Virosphere Using Metagenomics. *PLOS Genet.* **9**, (2013).
- 321 16. Abe, T. *et al.* tRNADB-CE: tRNA gene database well-timed in the era of big sequence
322 data. *Front. Genet.* **5**, 1–7 (2014).
- 323 UniProt Consortium. "UniProt: a hub for protein information." *Nucleic acids research* (2014):
324 gku989.

325 **Supporting Information: RESULTS**

326

327 **Supplementary Table 1 (Table S1)**

328 Physico-chemical properties of silver nanoparticles used in this study. BPEI refers to the type
329 of AgNPs added in the mesocosms [branced poly(ethyleneimine)] and TEM refers to
330 transmission electron microscopy.

331

Coating	BPEI
Nominal diameter	60
Diameter (TEM) (nm)	57.2±6.7
Surface Area (TEM) (m ² g ⁻¹)	9.7
Particle Concentration (particles mL ⁻¹)	2.1E+10
Hydrodynamic Diameter (nm)	98.2
Zeta Potential (mV)	46.2
pH of Solution	5.9

332

333 **Supplementary Table 2 (Table S2)**

334 Left column: Temporal changes in the concentration of Ag detected as dissolved Ag⁺ present
335 in the particulate fraction [inside or attached to microbial cells] in the size fraction 0.2-5.0 μm
336 determined by single particle ICP-MS.

337 Middle column: Temporal changes in the concentration of Ag detected as AgNPs in the
338 particulate fraction [inside or attached to the cells] in the size fractions 0.2-5.0 μm determined
339 by single particle ICP-MS.

340 Right column: Temporal changes in the concentration of total Ag detected in the size fraction
341 >5 μm determined by conventional ICP-MS following microwave digestion. Each data point is
342 the result of one measurement (mesocosm +NP1) and is given in ng Ag L⁻¹.

Day	Ag detected as dissolved Ag ⁺ (0.2-5.0 μm)	Ag detected as AgNPs (0.2-5 μm)	Total Ag detected (>5 μm)
2	8.63E-04	0.90	3.71
4	2.14E-03	1.86	18.69
8	8.61E-04	1.67	32.70
10	3.09E-03	2.57	33.84
13	5.71E-03	4.04	67.14
26	1.14E-03	0.84	16.40
33	2.49E-04	1.27	12.25

344 **Supplementary Table 3 (Table S3)**

345 Temporal changes in the concentration of >5.0, 2.0-5.0 and 0.2-2.0 μm chlorophyll *a* (Chl *a*),
346 the pico- (0.2-2.0 μm) and nano/micro (>2.0) primary production, the percentage of high,
347 medium and low DNA content virus-like particles (HDNA-v, MDNA-v, LDNA-v,
348 respectively), the percentage of high DNA content bacteria (HDNA-b) and the percentage of
349 “active” bacteria. The first table corresponds to the control mesocosms and the second table to
350 +NP mesocosms at experimental days D-1 to D32. Data are the mean value \pm standard deviation
351 of three replicated mesocosm.

Day	Chl <i>a</i>			Primary production		Virus-like particles			Bacteria	
	(µg L ⁻¹)			(mg C L ⁻¹ h ⁻¹)		(%)			(%)	
	>5.0	2.0-5.0	0.2-2.0	>2.0	0.2-2.0	HDNA- v	MDNA- v	LDNA- v	HDNA-b	active
-1	0.02	0.01	0.04			1 ±0.04	14 ±0.2	85 ± 0.3	84 ± 1	61±0.1
0	0.02±0.01	0.02±0.01	0.10±0.02	0.58±0.08	0.62±0.26	2 ±0.1	18 ±2	80 ±2	84 ±1	46±4
1	0.03±0.02	0.03±0.01	0.20±0.04	1.40±0.42	1.28±0.56	2±0.2	17 ±2	82 ±2	69 ±4	39±6
2	0.07±0.04	0.11±0.04	0.33±0.10	2.11±1.20	2.38±0.48	3 ±0.2	18 ±3	80 ±3	57 ±1	50±2
3	0.09±0.05	0.07±0.003	0.26±0.05			3 ±0.1	19 ±2	79 ±2	52 ±1	49±2
4	0.05±0.02	0.05±0.01	0.14±0.01	1.71±0.31	0.57±0.45	4 ±0.1	19 ±1	78 ±1	51 ±1	46±2
5	0.08±0.01	0.03±0.02	0.06±0.01			4 ±0.2	19 ±1	80 ±1	44±6	57±7
6	0.06±0.01	0.01±0.01	0.04±0.002	0.79±0.25	0.47±0.28	3 ±0.4	15 ±5	84 ±5	65±10	71±1
7	0.05±0.02	0.01±0.002	0.06±0.02			3 ±0.2	9 ±0.3	90 ±0.1	66 ±3	77±3
8	0.06±0.01	0.01±0.004	0.06±0.02	1.07±0.10	0.35±0.45	3 ±0.4	9 ±1	90 ±2	72 ±3	84±1
9	0.04±0.004	0.01±0.002	0.07±0.01			3 ±0.2	11 ±2	88 ±2	63 ±10	89±2

352	10	0.04±0.02	0.02±0.003	0.06±0.01			2 ±1	8 ±2	92 ±3	58 ±11	82±1
353	11	0.07±0.01	0.02±0.002	0.08±0.005	0.75±0.14	0.70±0.50	3 ±1	10 ±1	89 ±1		85±2
	25	0.03±0.02	0.01±0.001	0.03±0.01			3 ±1	11 ±1	86 ±1	60 ±4	85±3
	32	0.01±0.001	0.01±0.001	0.04±0.01			3±1	14±1	84±1	59 ±14	79±5

Day	Chl <i>a</i> ($\mu\text{g L}^{-1}$)			Primary production ($\text{mg C L}^{-1} \text{h}^{-1}$)		Virus-like particles (%)			Bacteria (%)	
	>5.0	2.0-5.0	0.2-2.0	>2.0	0.2-2.0	HDNA- v	MDNA- v	LDNA- v	HDNA-b	active
-1	0.02	0.01	0.04			1 \pm 0.04	14 \pm 0.2	85 \pm 0.3	84 \pm 1	64 \pm 0.1
0	0.02 \pm 0.004	0.02 \pm 0.01	0.09 \pm 0.002	0.40 \pm 0.10	1.18 \pm 0.32				85 \pm 1	43 \pm 2
1	0.03 \pm 0.01	0.03 \pm 0.01	0.21 \pm 0.03	1.22 \pm 0.30	1.38 \pm 0.46	2 \pm 0.2	17 \pm 1	82 \pm 1	67 \pm 4	40 \pm 4
2	0.06 \pm 0.03	0.09 \pm 0.05	0.31 \pm 0.06	2.17 \pm 1.09	2.22 \pm 0.84	3 \pm 0.1	17 \pm 3	81 \pm 3	58 \pm 3	36 \pm 16
3	0.08 \pm 0.04	0.08 \pm 0.004	0.27 \pm 0.06			3 \pm 0.1	17 \pm 0.1	82 \pm 0.1	54 \pm 1	47 \pm 0.1
4	0.04 \pm 0.02	0.05 \pm 0.01	0.16 \pm 0.01	1.38 \pm 0.15	0.83 \pm 0.43	3 \pm 0.3	19 \pm 1	79 \pm 1	52 \pm 2	46 \pm 4
5	0.05 \pm 0.02	0.03 \pm 0.01	0.09 \pm 0.03			4 \pm 0.1	18 \pm 0.1	80 \pm 0.1	39 \pm 8	54 \pm 3
6	0.05 \pm 0.02	0.01 \pm 0.003	0.05 \pm 0.004	0.74 \pm 0.16	0.38 \pm 0.11	3 \pm 0.2	16 \pm 1	83 \pm 1	65 \pm 10	71 \pm 0.2
7	0.04 \pm 0.02	0.02 \pm 0.003	0.04 \pm 0.002			3 \pm 1	8 \pm 1	91 \pm 0.3	62 \pm 9	75 \pm 4
8	0.06 \pm 0.03	0.02 \pm 0.01	0.05 \pm 0.01	0.65 \pm 0.63	0.88 \pm 0.46	2 \pm 0.5	8 \pm 1	92 \pm 2	73 \pm 1	77 \pm 2
9	0.04 \pm 0.003	0.02 \pm 0.01	0.06 \pm 0.01			3 \pm 1	11 \pm 1	88 \pm 2	67 \pm 6	89 \pm 1

354

10	0.06 ± 0.005	0.02 ± 0.01	0.07 ± 0.005			2 ± 1	9 ± 1	91 ± 1	57 ± 14	81 ± 1
11	0.06 ± 0.01	0.02 ± 0.004	0.08 ± 0.005	1.24 ± 0.25	0.27 ± 0.29	2 ± 0.4	10 ± 1	90 ± 1		83 ± 1
25	0.03 ± 0.005	0.01 ± 0.003	0.02 ± 0.002			3 ± 1	11 ± 0.5	86 ± 1	60 ± 4	84 ± 2
32	0.02 ± 0.01	0.01 ± 0.01	0.04 ± 0.01			3 ± 0.4	13 ± 1	84 ± 1	79 ± 45	76 ± 4

355 **Supplementary Table 4 (Table S4)**

356 Results of the PERMANOVA tests for the bacterial community patterns on the family (upper)
 357 and genus (lower) levels considering controls and +NP treatments. Factors: “treatment” and
 358 “time”.

359

Source	df	SS	MS	Pseudo-F	P(perm)	Unique perms
Treatment	1	4730	4730.0	1.476	0.103	999
Time	4	17950	4487.5	1.400	0.013	998
Treatment x Time	4	17444	4360.9	1.361	0.012	997
Residuals	12	38453	3204.4			
Total	21	78493				

360

361

Source	df	SS	MS	Pseudo-F	P(perm)	Unique perms
Treatment	1	4651	4651.8	1.468	0.079	997
Time	4	17606	4401.4	1.389	0.018	996
Treatment x Time	4	16257	4064.1	1.282	0.067	998
Residuals	12	38033	3169.4			
Total	21	76839				

362

363 **Supplementary Table 5 (Table S5)**

364 The relative abundance of the different categories of hypothetical proteins predicted by the viral
 365 genomes in the mesocosms over time. C refers to the control mesocosms and +NP to the
 366 mesocosms that received silver nanoparticles. Data derive from single viromes that were
 367 generated by merging the three replicated mesocosms before sequencing.

Hypothetical Protein Categories	D0	D5		D11		D25		D32	
		C	+NP	C	+NP	C	+NP	C	+NP
Amino acid transport and metabolism	0.4%	0.7%	1.0%	0.4%	0.7%	0.3%	0.6%	0.4%	0.8%
Carbohydrate transport and metabolism	0.0%	1.8%	2.4%	1.6%	2.0%	2.2%	2.9%	2.6%	2.0%
Cell wall membrane envelope biogenesis	2.7%	2.9%	3.0%	3.1%	3.5%	3.9%	2.3%	2.3%	2.8%
DNA packaging	3.5%	1.7%	1.3%	1.1%	1.5%	1.7%	1.0%	1.0%	1.3%
DNA synthesis and repair	17.8%	8.9%	8.6%	19.0%	17.4%	9.2%	16.3%	17.9%	18.9%
Energy production and conversion	7.2%	7.1%	8.4%	7.6%	6.7%	8.2%	9.8%	8.7%	7.3%
General function known	1.7%	1.7%	1.5%	1.3%	1.2%	2.2%	1.0%	0.7%	1.1%
Nucleotide transport and metabolism	12.3%	15.0%	15.2%	13.1%	14.2%	16.4%	14.4%	14.1%	12.5%
Post translational modification. protein turnover. chaperones	7.8%	9.8%	9.3%	7.6%	7.4%	8.4%	7.5%	7.7%	7.8%
Replication recombination and repair	22.0%	26.0%	24.2%	20.9%	20.8%	23.9%	18.4%	20.6%	23.2%
Signal transduction mechanisms	0.0%	0.1%	0.1%	0.0%	0.1%	0.0%	0.2%	0.0%	0.0%
Virus structure	15.5%	15.3%	16.6%	14.4%	14.6%	15.0%	14.0%	12.2%	13.3%
Inorganic ion transport and metabolism	0.0%	0.1%	0.4%	0.4%	0.1%	0.1%	0.2%	0.3%	0.1%
Translation. ribosomal structure and biogenesis	3.5%	3.8%	3.3%	4.1%	4.0%	3.5%	5.0%	3.9%	3.8%
Transcription	1.6%	0.9%	1.1%	1.6%	1.7%	0.7%	1.5%	1.3%	1.2%
Unknown function	4.1%	4.1%	3.6%	3.6%	3.9%	4.3%	4.6%	6.0%	3.8%

369 **Supplementary Table 6 (Table S6)**

370 Results of the PERMANOVA tests for the dinoflagellate (first) and diatom (second) community

371 composition considering controls and +NP treatments. Factors: “treatment” and “time”.

Source	df	SS	MS	Pseudo-F	P(perm)	Unique perms
Treatment	1	78	78.96	0.634	0.616	999
Time	8	23000	2875	23.085	0.001	996
Treatment x Time	8	1100	137.52	1.104	0.395	999
Residuals	36	4483	124.54			
Total	53	28663				

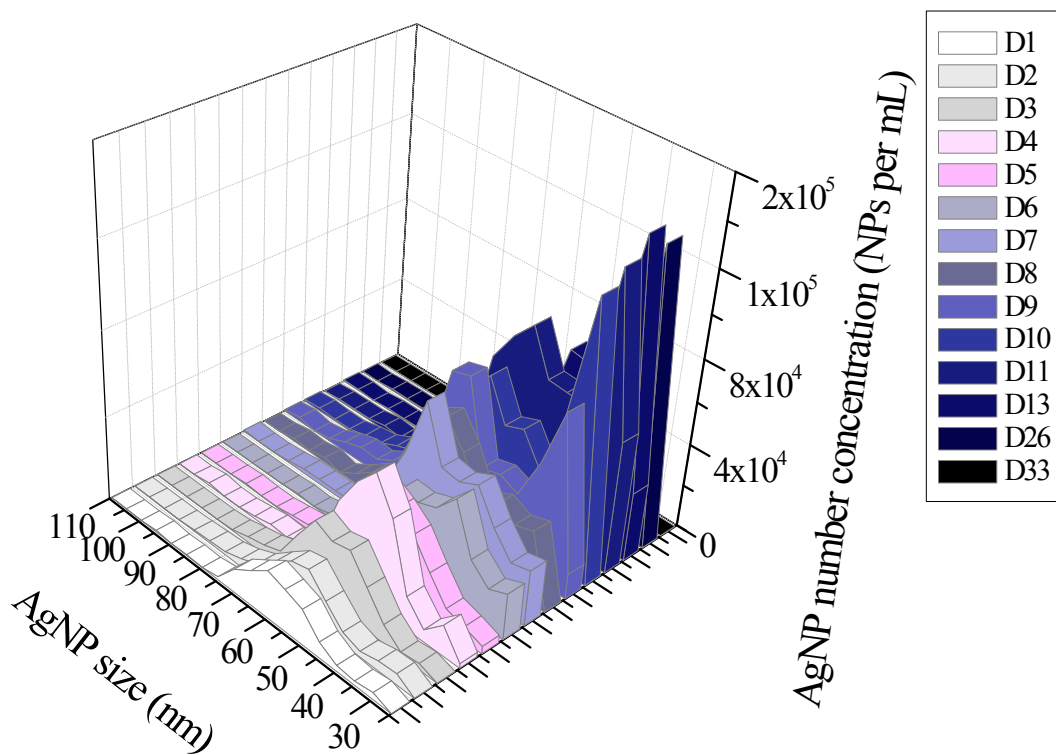
372

Source	df	SS	MS	Pseudo-F	P(perm)	Unique perms
Treatment	1	146	146.23	0.167	0.951	999
Time	8	39712	4964.00	5.669	0.001	996
Treatment x Time	8	5971	746.45	0.852	0.749	999
Residuals	36	31523	875.63			
Total	53	77353				

373

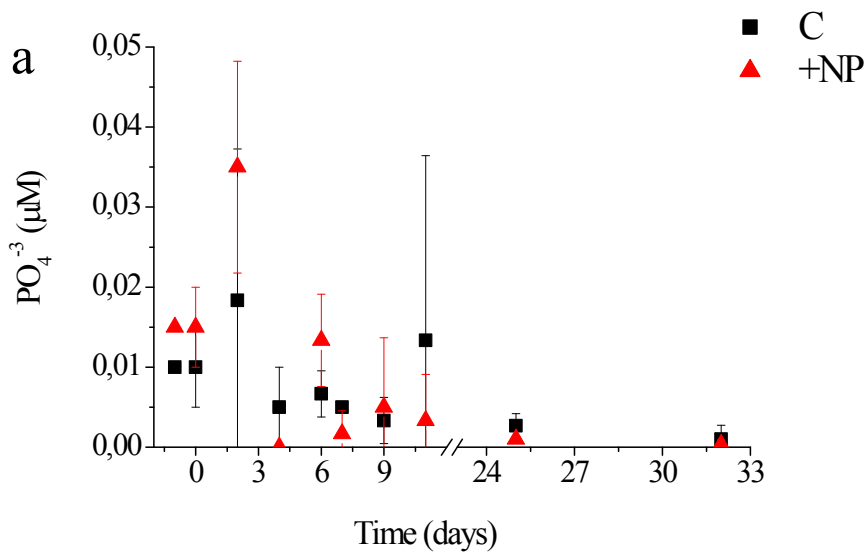
374 **Supplementary Figure 1 (Figure S1)**

375 Temporal changes in the size distribution of AgNP number concentration (number mL⁻¹) over
376 time. Data derive from the mean of three replicated mesocosms..

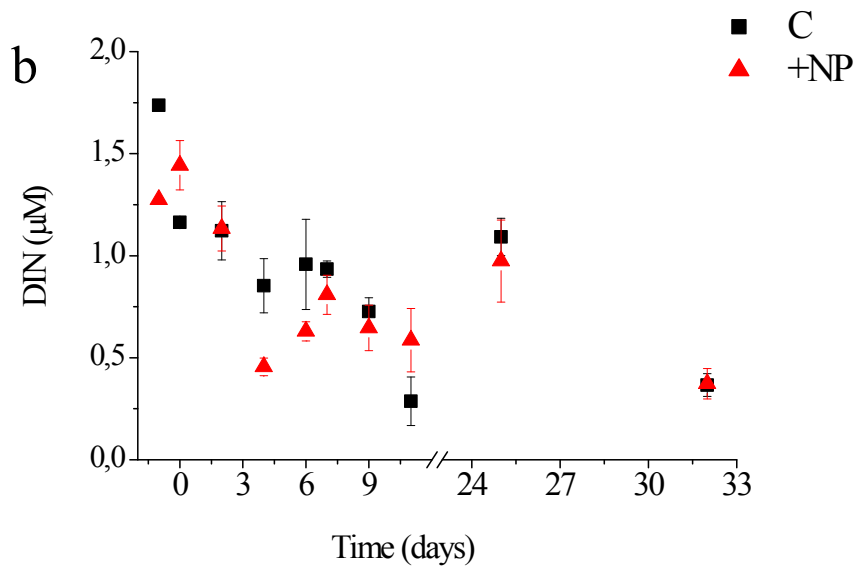


378 **Supplementary Figure 2 (Figure S2)**

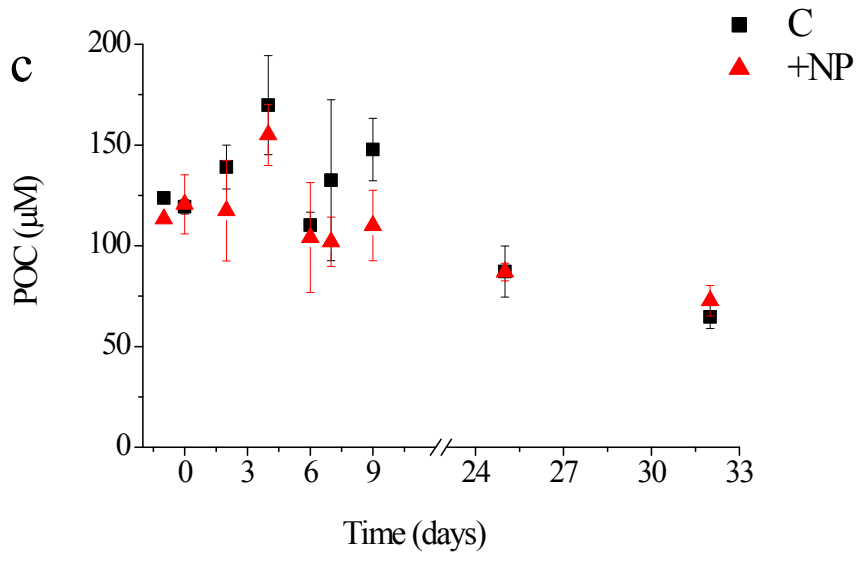
379 Temporal changes in the concentrations of phosphate (a: PO_4^{3-}), dissolved total inorganic
380 nitrogen (b: DIN), particulate organic carbon (c: POC), particulate organic nitrogen (d: PON),
381 total organic carbon (e: TOC), total chlorophyll *a* (f: Chl *a*) and reactive oxygen species (g:
382 presented in relative fluorescence units in logarithmic scale) in the mesocosms over time. C
383 refers to the control mesocosms and +NP to the mesocosms that received silver. Data derive
384 from the mean \pm standard deviation of triplicate mesocosms.



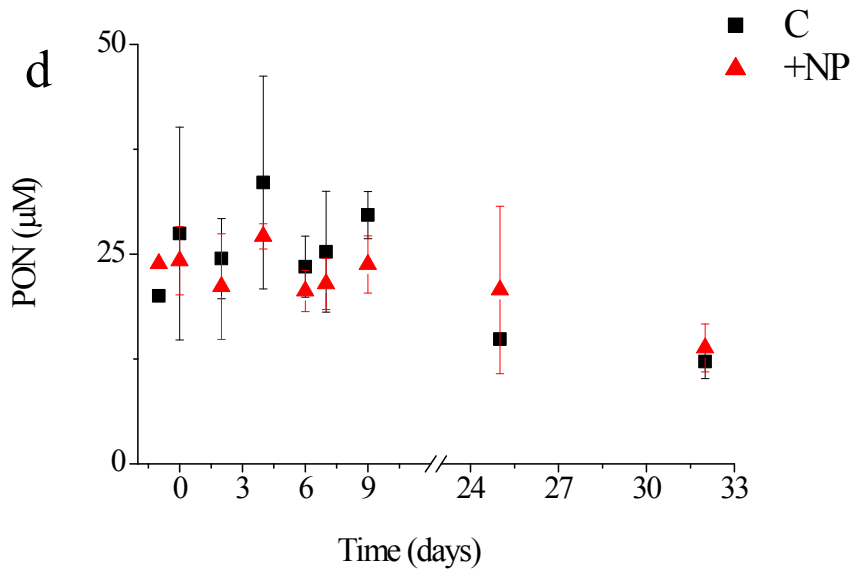
385



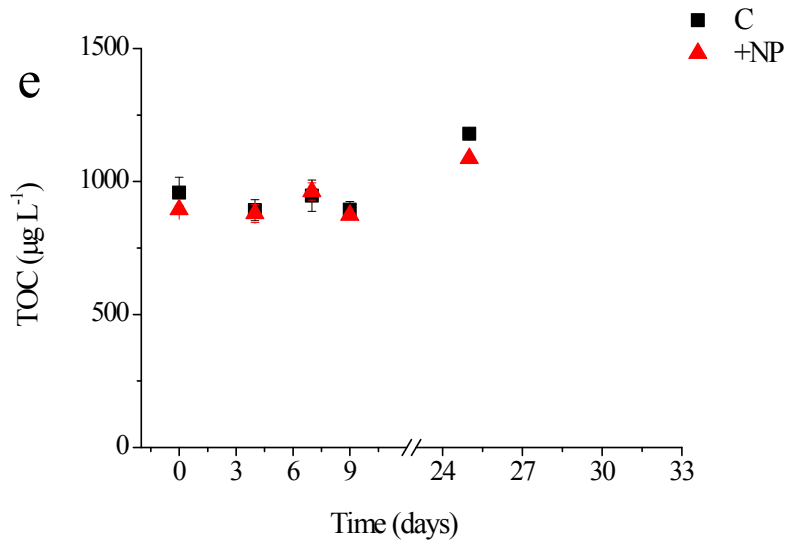
386



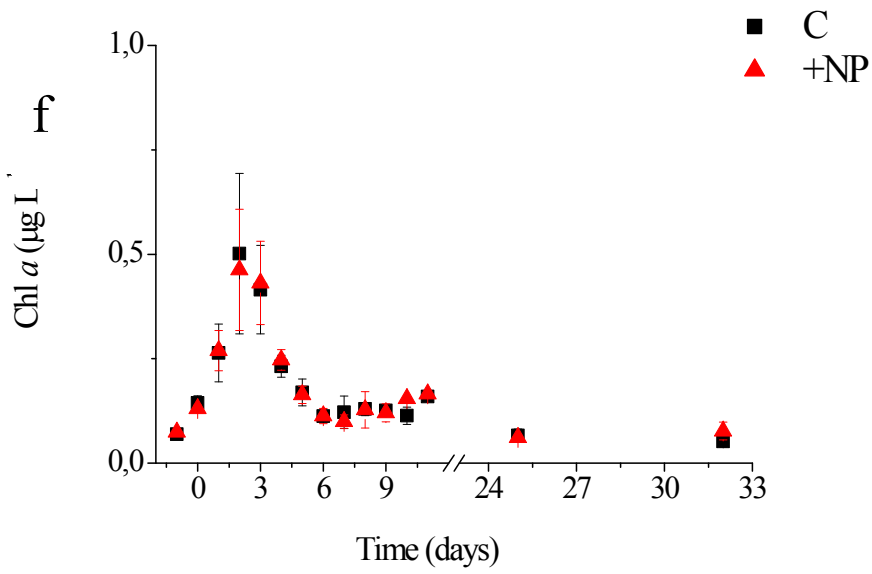
387



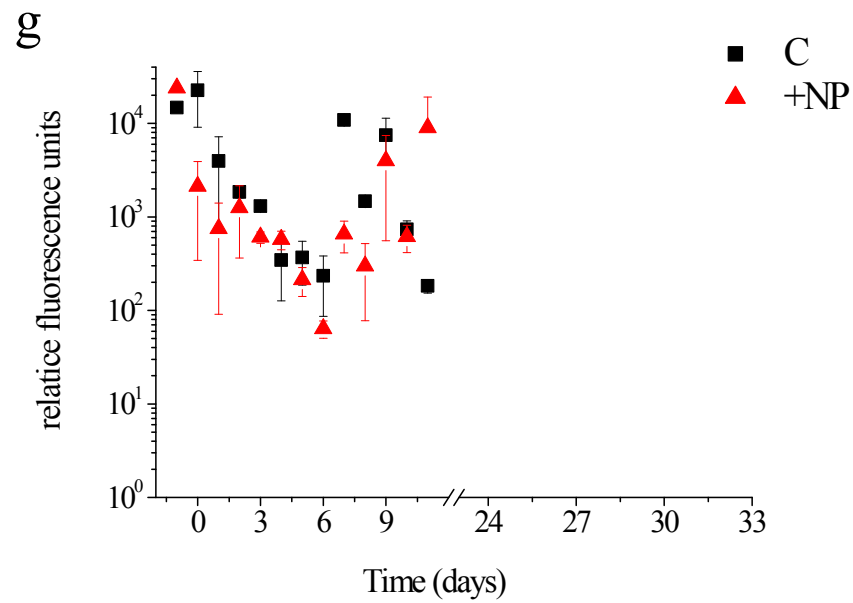
388



389



390

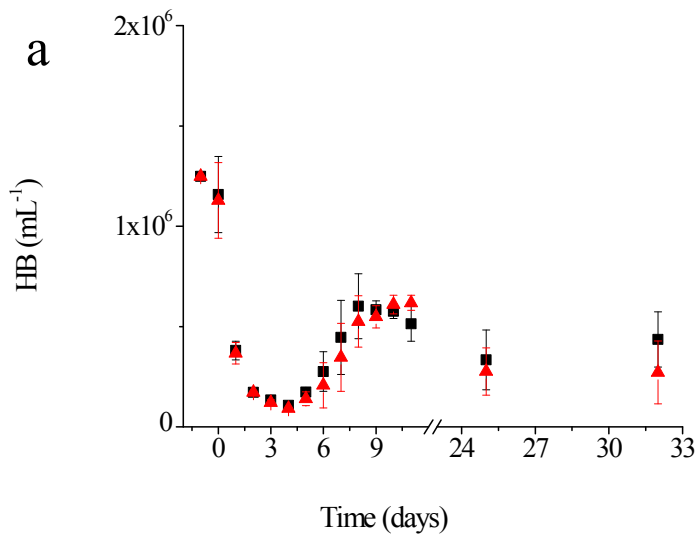


391

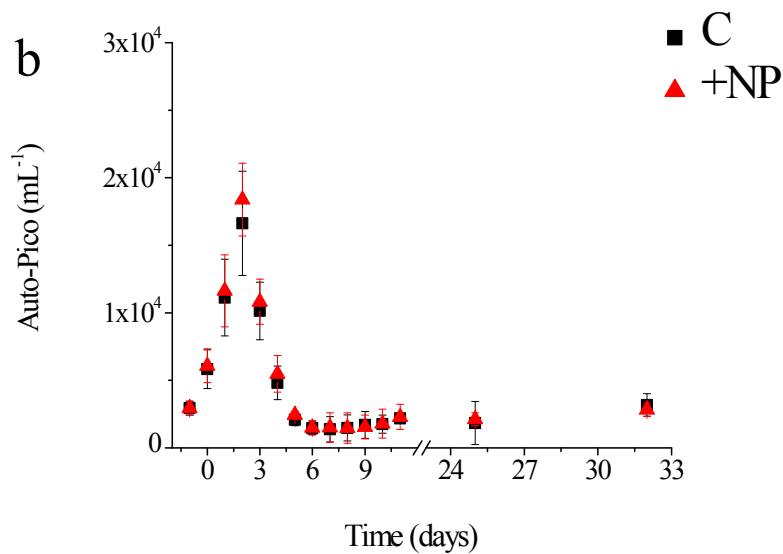
392 **Supplementary Figure 3 (Figure S3)**

393 Temporal changes in the abundances of heterotrophic bacteria (a: HB), autotrophic pico- and
394 nano- eukaryotes (b: Auto-Pico and c: Auto-Nano, respectively), heterotrophic pico- and nano-
395 eukaryotes (d: Hetero-Pico and e: Hetero-Nano, respectively), dinoflagellates (f) and ciliates
396 (g) in the mesocosms over time. C refers to the control mesocosms and +NP to the mesocosms
397 that received silver nanoparticles. Data derive from the mean \pm standard deviation of triplicate
398 mesocosms.

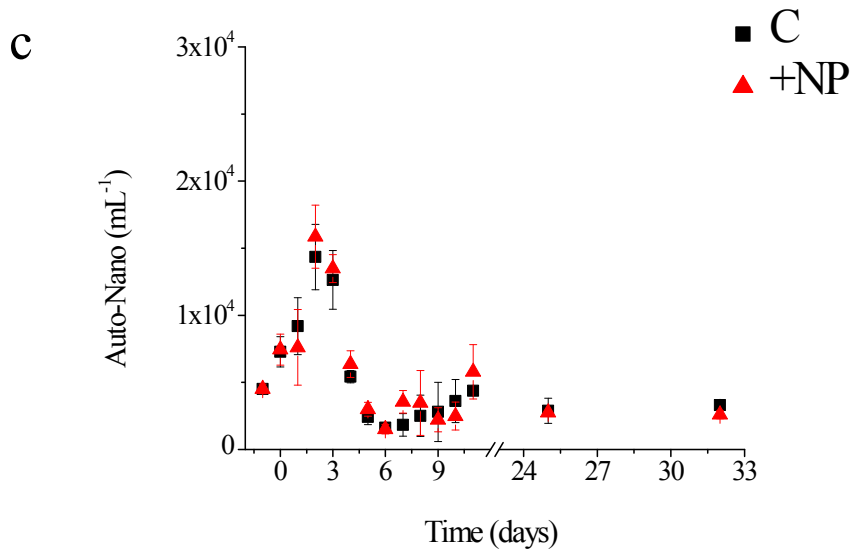
399



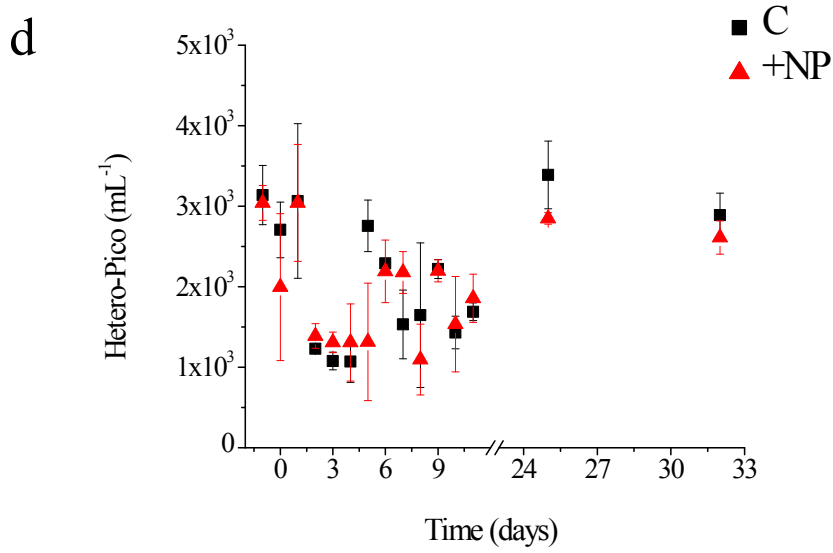
400



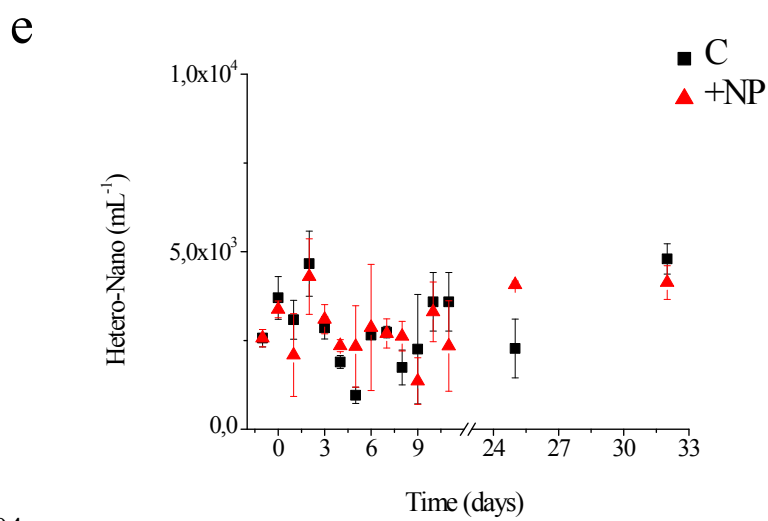
401



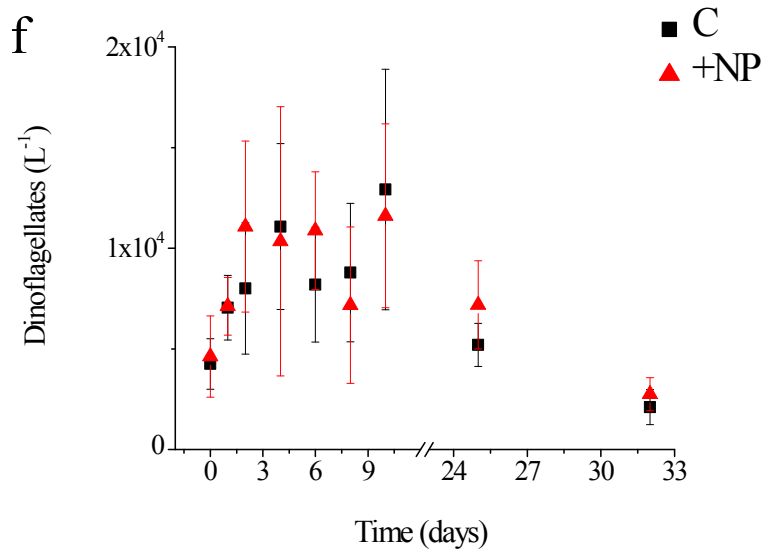
402



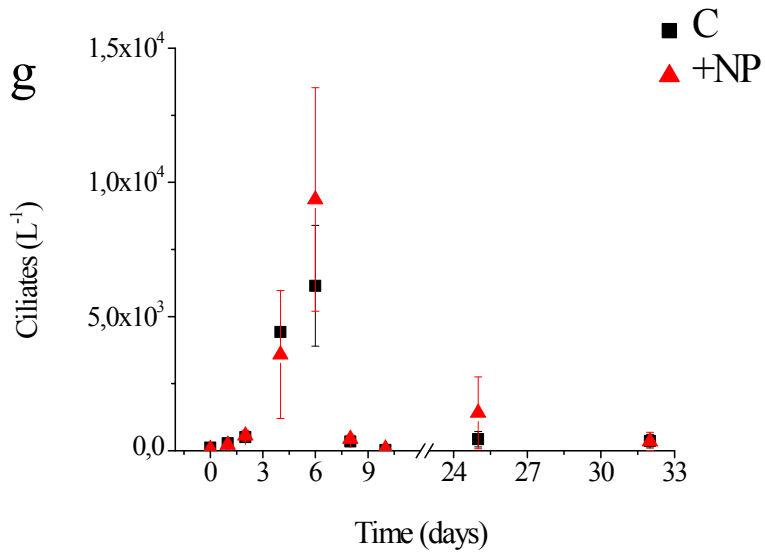
403



404



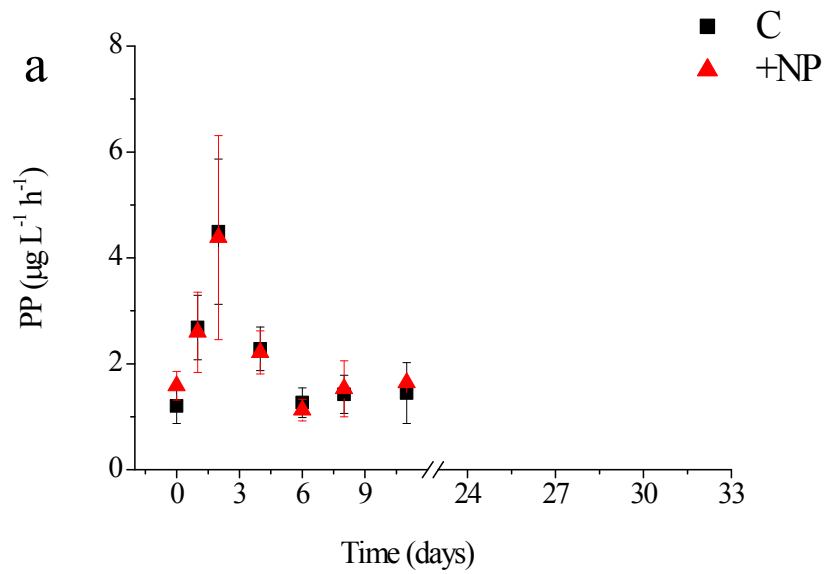
405



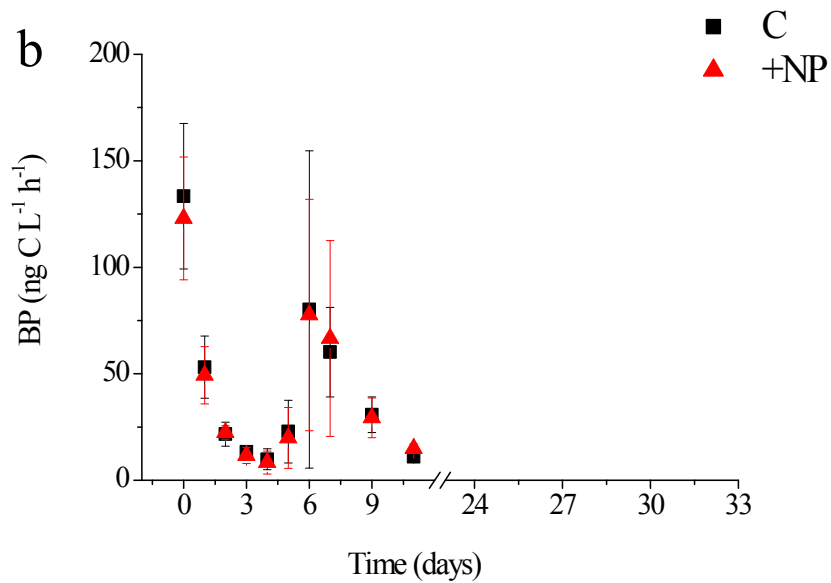
406

407 **Supplementary Figure 4 (Figure S4)**

408 Temporal changes in primary (a: PP) and heterotrophic bacterial (b: BP) production rates in the
409 mesocosms over time. C refers to the control mesocosms and +NP to the mesocosms that
410 received silver nanoparticles. Data derive from the mean \pm standard deviation of triplicate
411 mesocosms.



412



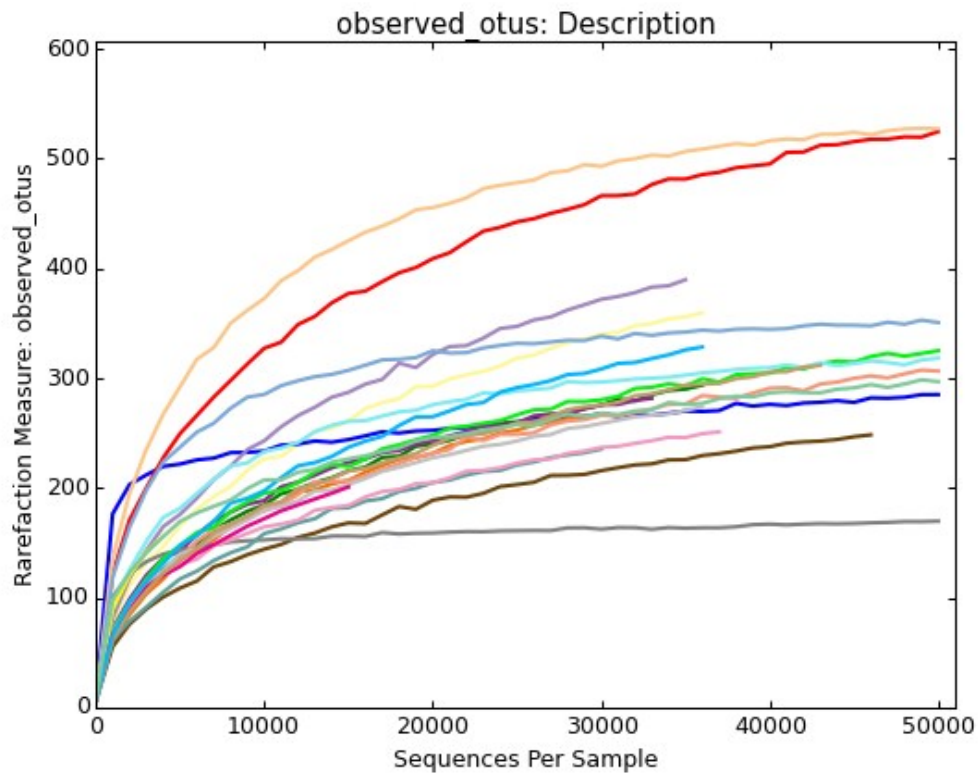
413

414

415 **Supplementary Figure 5 (Figure S5)**

416 Rarefaction curve plot for all samples. Each line represents a different sample. OTU:

417 operational taxonomic unit.

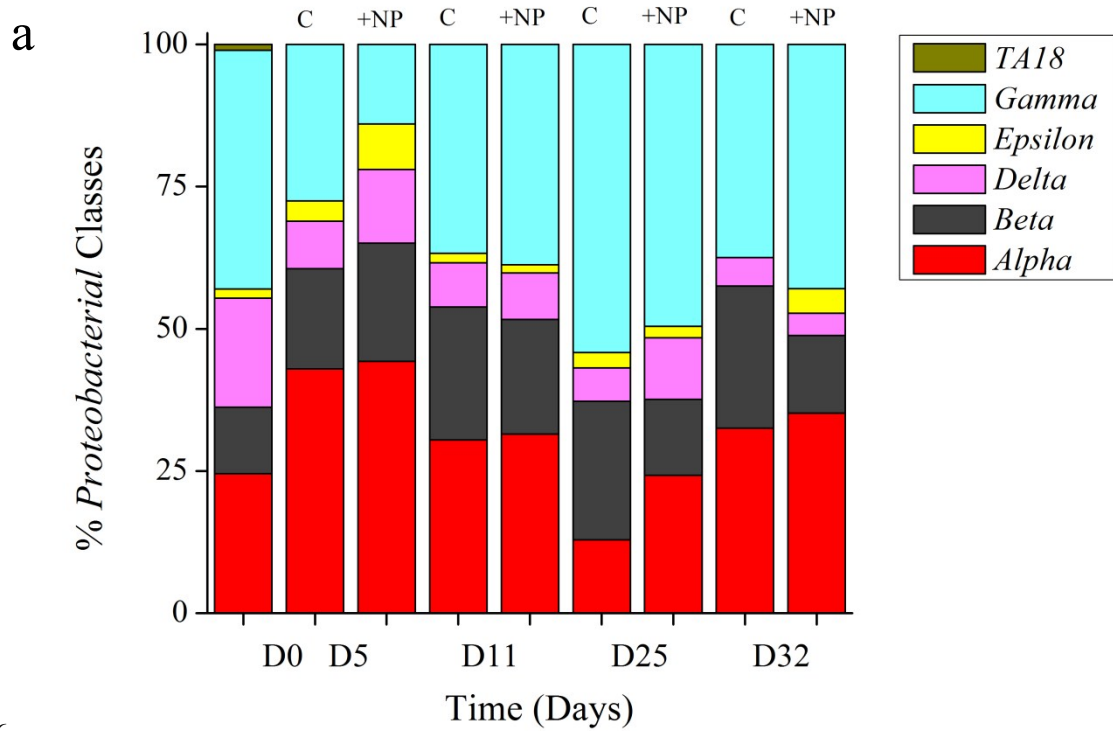


418

419

421 **Supplementary Figure 6 (Figure S6)**

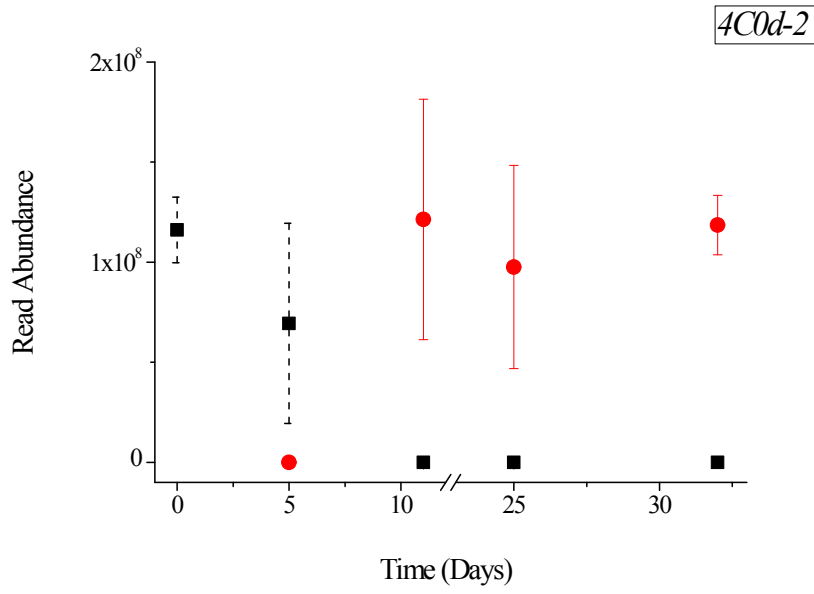
422 Temporal changes in the relative abundances of (a) *Proteobacterial* classes and (b) *4C0d-2*
423 class and (c) *Synechococcophycidae* class in the mesocosms over time. C refers to the control
424 mesocosms and +NP to the mesocosms that received silver nanoparticles. Data derive from the
425 mean of triplicate mesocosms, apart from D0 that derives from the mean of C1 and +NP1.



426

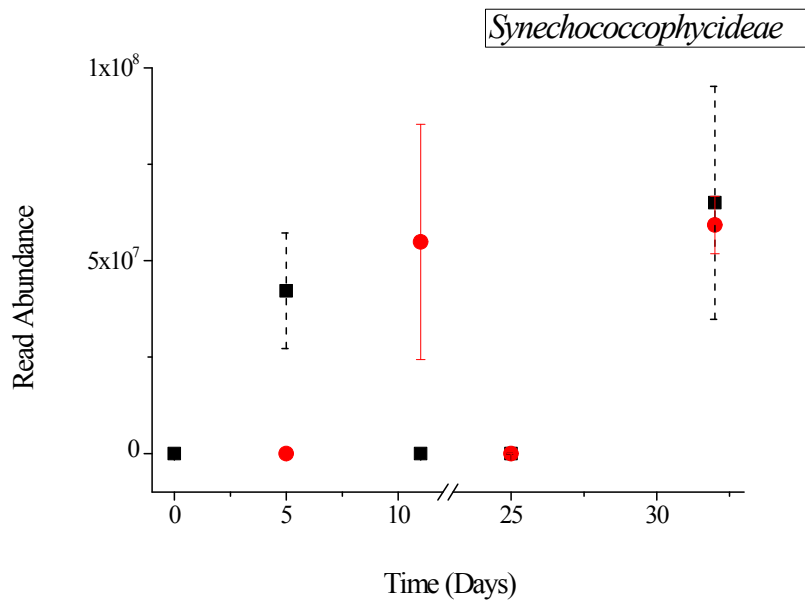
427

b



428

c



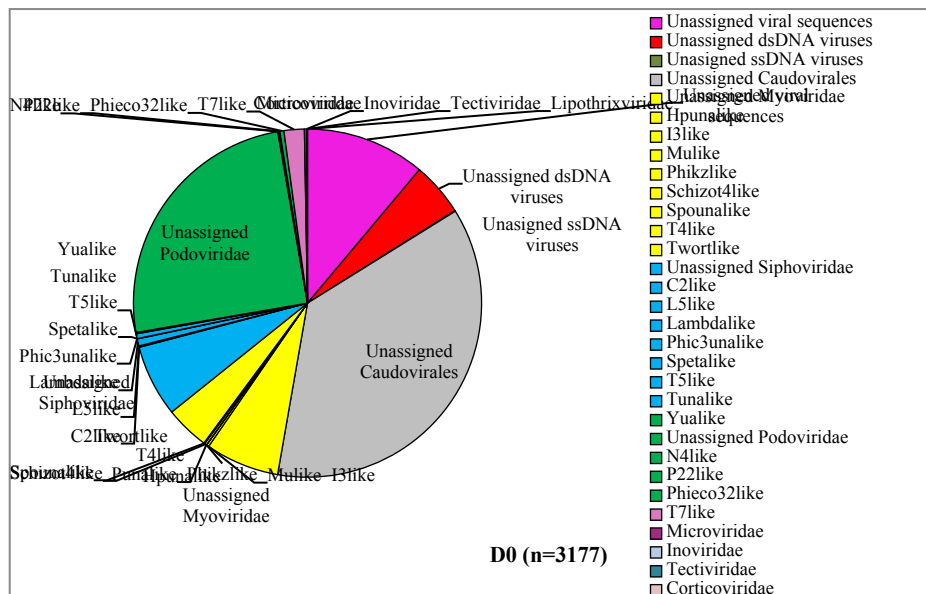
430

431

432 **Supplementary Figure 7 (Figure S7)**

433 Taxonomic affiliation of the viral sequencing data in the mesocosms. Numbers of sequences
 434 and sample names are shown in parentheses. Data derive from single viromes that were
 435 generated by pooling triplicate mesocosms before sequencing. C refers to the control
 436 mesocosms and +NP to the mesocosms that received silver nanoparticles.

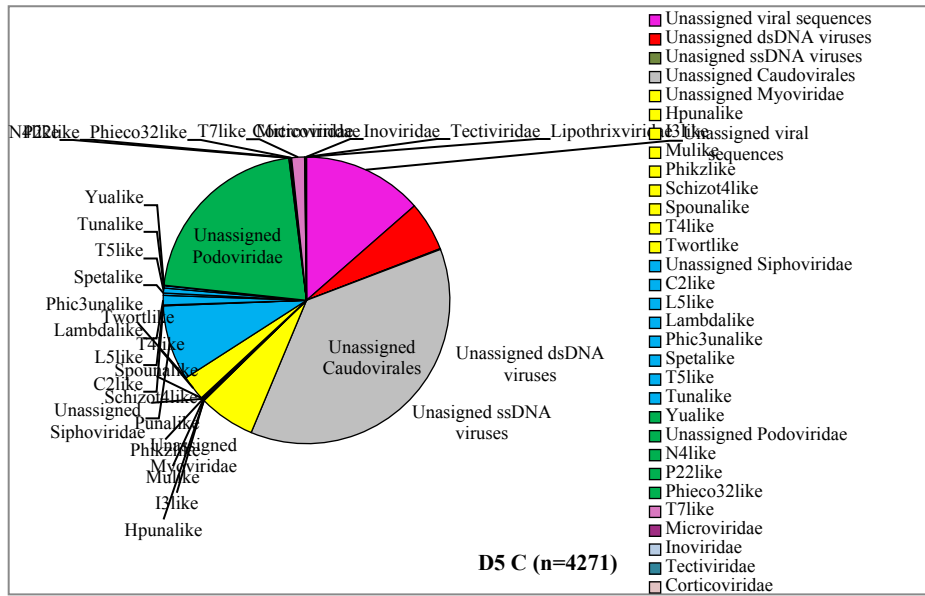
437



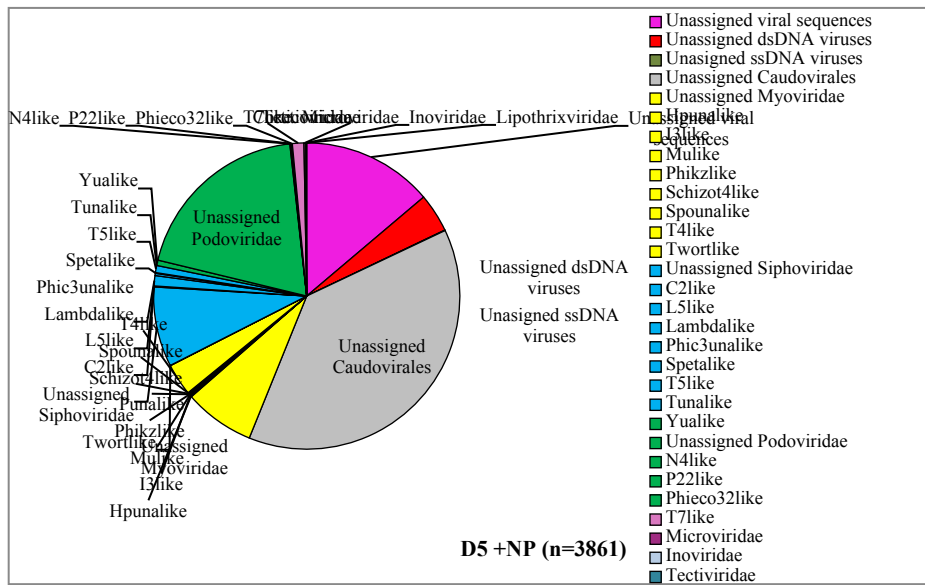
438

439

440



441

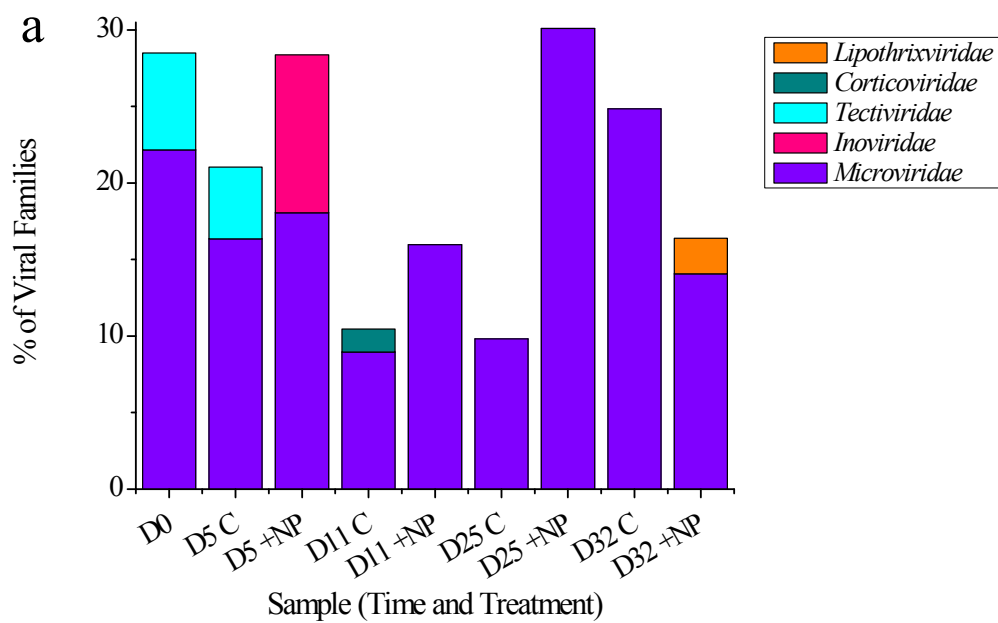


442

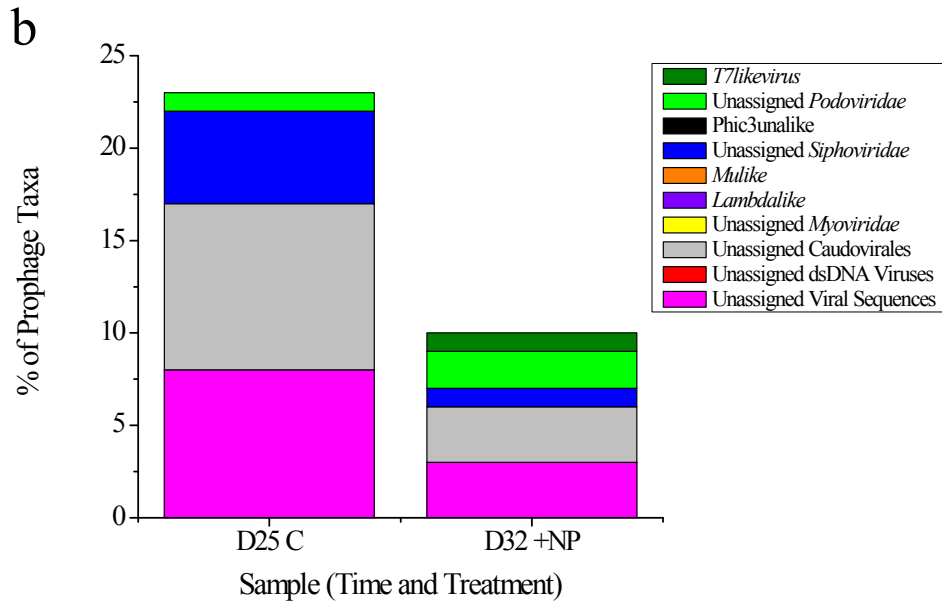
443

452 **Supplementary Figure 8 (Figure S8)**

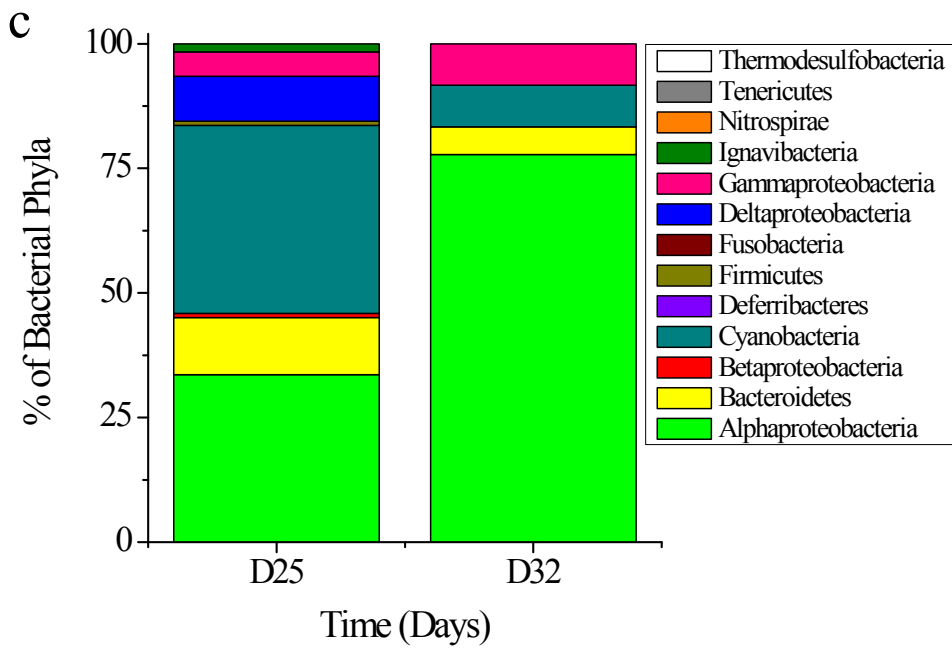
453 Temporal changes in the abundances of the (a) rarest lytic viral families over time, (b) lysogenic
454 viral sequences and (c) relative abundance of putative hosts of lysogenic viruses on D25 and
455 D32. Data derive from single viromes that were generated by pooling triplicate mesocosms
456 before sequencing. C refers to the control mesocosms and +NP to the mesocosms that received
457 silver nanoparticles.



458



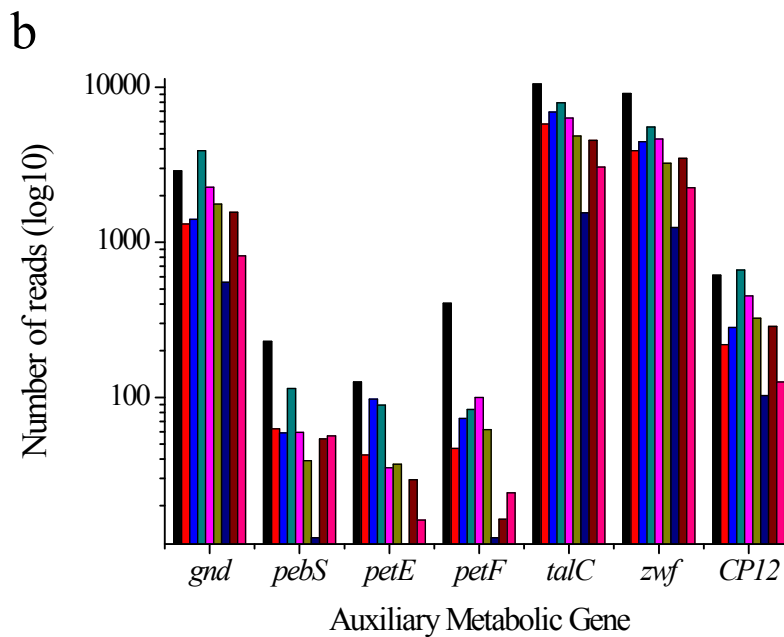
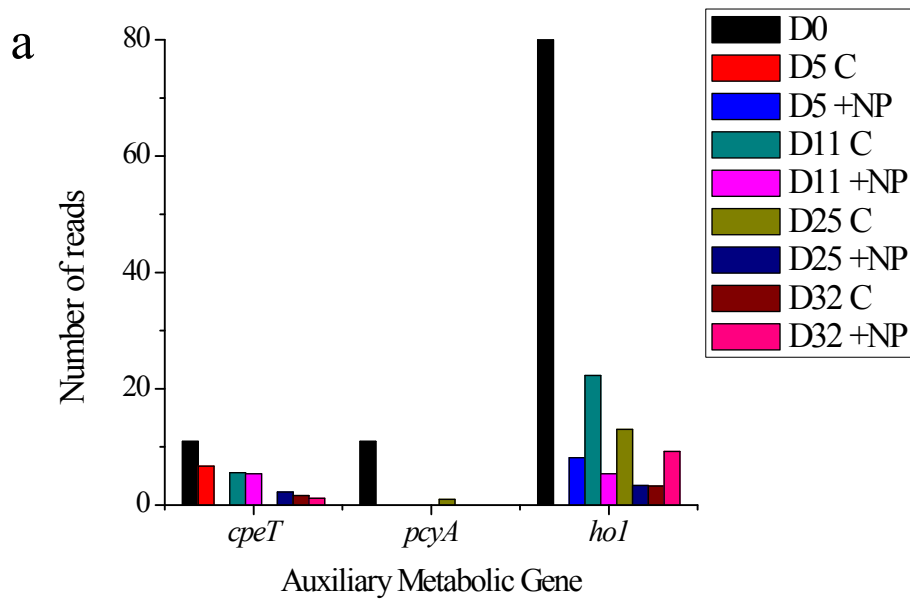
459



460

461 **Supplementary Figure 9 (Figure S9)**

462 Temporal changes in the abundances of auxiliary metabolic genes related to host photosynthesis
 463 (a; *cpeT*, *pcyA* and *hol* and b; *gnd*, *pebS*, *petE*, *petF*, *talC*, *zwf* genes) in the mesocosms over
 464 time. Data derive from single viromes that were generated by pooling triplicate mesocosms
 465 before sequencing. C refers to the control mesocosms and +NP to the mesocosms that received
 466 silver nanoparticles.



469 *Noise removal processing of the 16S rRNA sequences*

470 A total of 3.060.263 paired-end raw 16S rRNA gene sequences were obtained from the MiSeq
471 platform. After the removal of low-quality sequences (~25%), chimeras (~20%) and OTUs with
472 unassigned taxonomy or assigned to Archaea (363 OTUs), the final OTU table included
473 1.434.253 sequences that were affiliated to 1359 OTUs. The number of sequences per sample
474 varied from 15.621 (D32 C2) to 166.466 (D25 C2) with an average of 65.197 sequences per
475 sample.

476 *Bacterial community composition*

477 On D0, the dominant OTUs were assigned to *Proteobacteria* (45.8%) and the next most
478 abundant ones to *Bacteroidetes* (10.7%), *Firmicutes* (9.7%) and *Actinobacteria* (7.1%). A
479 common decrease of the OTUs abundance assigned to the class *TA18* was seen in both C and
480 +NP from D0 to D5; *TA18* class remained absent until the end of the experiment in all tanks.
481 The percentage of *Deltaproteobacteria* varied little with time until D11, and on D25 and D32
482 it was lower in the controls than in +NP (6.1 and 0.00% vs. 12.1 and 4.1%, respectively).
483 *Betaproteobacterial* proportion was rather stable in all mesocosms in terms of percentage
484 contribution, and a mild difference was seen only on D25 and D32 between controls and
485 treatments (lower in +NP). Similarly, *Alphaproteobacterial* contribution was also the same
486 between the different mesocosms, except for D25 when it was higher in +NP. Within
487 *Gammaproteobacteria*, the orders of *Alteromonadales*, *Chromatiales*, *Legionales*,
488 *Oceanospirales*, *Pseudomonadales* and *Xanthomonadales*, and within *Delataproteobacteria*,
489 the orders of *Bdellovibrionales*, *Myxococcales* and *Sva0853* were absent in +NP on D5
490 compared to C. Rare phyla, including *Elusimicrobia*, *Fusobacteria* and *TM7*, were absent in all
491 tanks except for the initial condition on D0. *SBR1093*, *Omnitrophica* and *Gracilibacteria* phyla
492 exhibited higher percentage only on D5 in +NP compared to C, while *Parcubacteria* had a
493 minor contribution to the total reads, which was always lower in +NP (0.7%) compared to the
494 controls (1.8%).

495 *Viral community composition*

496 Virome processing resulted in the prediction of 38.592 high-confidence curated viral sequences.
497 Table S6 shows the proportion of circular contigs, prophage genes (integrated into a microbial
498 contig), lytic genes (ds and ssDNA viruses, with no RNA stage), unclassified viral sequences
499 with no microbial gene, virophages, the percentage of sequences not assigned to viruses, and
500 the number of hypothetical proteins predicted by the viral sequences in the mesocosms over
501 time. Among the predicted genes 26.1-37.7% did not have a viral database match. On average,
502 83.4% (± 1.5) of the rest of the genes had a hit to the tailed *Caudovirales* phages, while 12.1%
503 (± 1.1) could not be assigned to any known viral group (highest percentage on D5).

504 *Siphoviridae* reads matched larger proportion in +NP compared to C during several days.
505 Within *Siphoviridae*, the genera *Lambdalike*, *T5like*, *Tunalike* and *Yualike* exhibited slightly
506 higher contributions in +NP than in the controls. *Podoviridae* had the opposite pattern, with
507 slightly lower percentages in +NP, with genera *N4like* and *T7like* being the most responsible
508 for this pattern. *Tectiviridae* was only present on D0 and D5 in the controls.

509 Prophage (i.e. lysogenic) sequences were detected on D5 and D11 in C and +NP, while on D25
510 and D32 they were detected only in C and +NP, respectively. The majority (65.0-87.0%) was
511 assigned to *Caudovirales*. Prophage genes assigned to *Mulike* viruses of the *Myoviridae* family
512 were absent from the +NP treatments on D5 and D11, in contrast to the controls that a small
513 number was detected. From the 38.592 viral sequences, a pool of 66.399 proteins was predicted.
514 Functional annotation was done with the dsDNA viruses' database of EggNOG. A range of 8-
515 10% hypothetical proteins was annotated. Among them, the majority was predicted to have
516 "replication, recombination and repair" role with a peak on D5 to 24.2-26.0% (Table S8).